Electronic States of Tetrahydrofurfuryl Alcohol (THFA) As Studied by VUV Spectroscopy and Ab Initio Calculations

ARTICLE *in* THE JOURNAL OF PHYSICAL CHEMISTRY A · APRIL 2014

Impact Factor: 2.69 · DOI: 10.1021/jp501634w · Source: PubMed

THE JOURNAL OF PHYSICAL CHEMISTRY A

Article

pubs.acs.org/JPCA

Electronic States of Tetrahydrofurfuryl Alcohol (THFA) As Studied by VUV Spectroscopy and Ab Initio Calculations

P. Limão-Vieira,*[,†] D. Duflot,[‡] M.-J. Hubin-Franskin,[§] J. Delwiche,[§] S. V. Hoffmann,[∥] L. Chiari,[⊥] D. B. Jones,[⊥] M. J. Brunger,[⊥,#] and M. C. A. Lopes[▽]

[†]Laboratório de Colisões Atómicas e Moleculares, CEFITEC, Departamento de Física, Faculdade de Ciências e Tecnologia, Universidade Nova de Lisboa, 2829-516 Caparica, Portugal

[‡]Laboratoire de Physique des Lasers, Atomes et Molécules (PhLAM), UMR CNRS 8523, Université Lille 1, Bât. P5 – USTL, F-59655 Villeneuve d'Ascq Cedex, France

[§]Départment de Chimie, Université de Liège, Institut de Chimie-Bât. B6C, allée de la Chimie 3, B-4000 Liège 1, Belgium

[∥]ISA, Department of Physics and Astronomy, Aarhus University, Ny Munkegade 120, DK-8000 Aarhus C, Denmark

[⊥]CaPS, Flinders University, GPO Box 2100, Adelaide, SA 5001, Australia

[#]Institute of Mathematical Sciences, University of Malaya, Kuala Lumpur 50603, Malaysia

[▽]Departamento de Física, Universidade de Juíz de Fora, Juíz de Fora 36036-330, MG Brazil

Supporting Information

ABSTRACT: The electronic spectroscopy of isolated tetrahydrofurfuryl alcohol (THFA) in the gas phase has been investigated using high-resolution photoabsorption spectroscopy in the 5.0–10.8 eV energy-range, with absolute cross-section measurements derived. The He(I) photoelectron spectrum was also collected to quantify ionization energies in the 9–16 eV spectral region. These experiments are supported by the first high-level ab initio calculations performed on the excited states of the neutral molecule and on the ground and excited state of the positive ion. The good agreement between the theoretical results and the measurements allows us to quantify for the first time the electronic-state spectroscopy of THFA. The present work also considers the question of the lowest energy conformers of the molecule and its population distribution at room temperature.

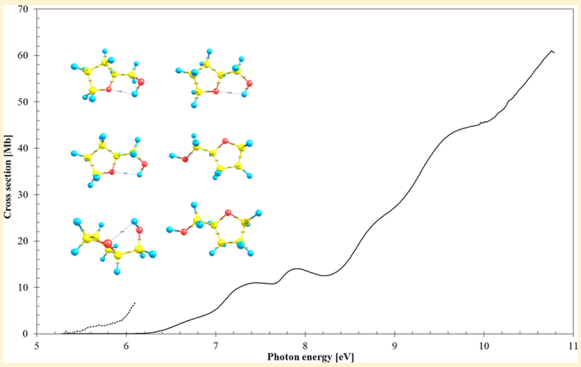

1. INTRODUCTION

The pioneering work of Sanche and coworkers,[1] on the resonant formation of DNA strand breaks triggered by low-energy electrons, has attracted considerable attention from the international community in regards to electron-[2] and photon-[3] induced decomposition processes in biologically relevant targets. Low-energy secondary electrons are also responsible for exciting biomolecular targets through inelastic collisions, meaning that electronic excitation may be attained. These excited states may then subsequently decay into the production of radicals whose chemical reactivity may strongly influence the local site chemistry. As such, a detailed comprehension of the underlying molecular mechanisms (e.g., the electronic state spectroscopy) is necessary if we are to develop a quantitative knowledge of radiation-induced damage in DNA/RNA and its constituents at the molecular level.[4,5]

Because of the considerable fragility of the sugar moiety against the nucleobases upon electron impact/transfer or photon absorption, several contributions have been reported (see, e.g., refs 6–8 and references therein). Tetrahydrofurfuryl alcohol (tetrahydro-2-furanmethanol) (THFA) has been recently studied by electron scattering[9−12] and electron impact ionization[13,14] methods and can be regarded as a transient structural form between tetrahydrofuran (THF) and deoxyribose, both of which have been investigated by photon, electron, positron, and neutral potassium impact.[15−28] We also note other structurally related ether and azole molecules that have been investigated in the context of the furan molecule.[29−31]

This work was partially engendered by the need to understand the spectroscopy of furanose-structured alcohol species and their role as biorelated molecules. Our knowledge of the VUV electronic state spectroscopy of THFA remains poorly quantified in a wide wavelength (λ) region; indeed as far as we are aware experimental information on such chemical

Special Issue: Franco Gianturco Festschrift

Received: February 14, 2014
Revised: April 17, 2014
Published: April 17, 2014

Table 1. Relative Energies (kcal/mol) of the Six Most Abundant Isomers of THFA Calculated without and with the Inclusion of Zero-Point Vibrational Energies Compared with Previous Works

	this work						33			34		
	MP2	MP2	MP2	MP2	MP2	MP2	G3MP2//B3LYP	B3LYP	B3LYP	MP2	HF	HF
	cc-pVTZ			aug-cc-pVDZ			6-311+G(2d,2p)			6-311++G**		
	ΔH (298 K)	+ZPE	no ZPE	ΔH (298 K)	+ZPE	no ZPE	ΔH (298 K)	+ZPE	no ZPE	no ZPE	+ZPE	no ZPE
A	0.05	0.01	0.10	0.12	0.07	0.18	0.12	0.08	0.00	0.2	0.0	0.0
B	0.65	0.61	0.68	0.50	0.47	0.53	0.35			0.6	0.1	0.2
C	0.00	0.00	0.00	0.00	0.00	0.00	0.00	0.00	0.04	0.0	0.3	0.2
D	0.74	0.70	0.78	0.59	0.55	0.62	0.43			0.7	0.4	0.4
E	2.94	2.69	3.15	2.60	2.35	2.79	2.32			3.0	1.5	1.8
F	2.59	2.39	2.80	2.31	2.11	2.50	2.08			2.7	1.6	1.9

data is mainly restricted to $\lambda \leq 248$ nm ($E \geq 6.2$ eV).[2] The relatively old data of Dickinson and Johnson[32] appear in a restricted energy region (6.2−9.9 eV) and at a modest resolution. Thus, one rationale for the present study is to extend that restricted range, here to 5.0−10.8 eV, to improve the resolution and also provide reliable absolute photoabsorption cross sections.

The molecular structure and conformations of THFA in the gas phase have been studied with quantum-chemical calculations[33] and electron diffraction,[34] with the most stable conformer stabilized by hydrogen bonding and with the O−H group located outside the ring with a distorted $_4T^3$ conformation.[34] Finally, we note that the vertical energies of the lowest ionic states of THFA (ground and first excited) have been determined by Allan et al.[9] using photoelectron spectroscopy (PES).

We report the results of an extensive study on the electronic state spectroscopy of THFA by high-resolution VUV photoabsorption and He(I) spectroscopies. In addition, results from ab initio theoretical calculations of the vertical excitation energies and oscillator strengths for the neutral electronic transitions are also given. The ionization energies (IEs) for the lowest ionic states are also estimated using different levels of theory. In the next section, we provide a brief summary of the structure and properties of THFA. In Section 3, we present a brief discussion of the experimental methods, and in Section 4 the computational details are described. Section 5 is devoted to presenting and discussing the results of our study with a comparison with other absolute photoabsorption cross sections being made where possible. Finally, some conclusions that can be drawn from this investigation are given in Section 6.

2. BRIEF SUMMARY OF THE STRUCTURE AND PROPERTIES OF THFA

THFA has the symmetry C_1 in its electronic ground state. The symmetry species available to a C_1 molecule is A and the calculated electron configuration of the outermost valence orbitals of the $\tilde{X}\ ^1A$ ground state is $(23a)^2\ (24a)^2\ (25a)^2\ (26a)^2\ (27a)^2\ (28a)^2$. Previous works[33,34] have shown that six isomeric conformers can have significant abundances at room temperature in the gas phase. (See section 4 for details of our computations.) The energies of these conformers are compared with previous work in Table 1. All methods, except Hartree−Fock, agree to predict that conformer C is the most stable, with conformer A barely less stable. Relative weights of the six most abundant isomers of THFA at room temperature (using enthalpy values) are shown in Table 2. Our results show that only conformers A−D are present at room temperature. These values differ significantly from the 84%/16% ratio for A and B used by Borisenko et al.[34] in the interpretation of their electron diffraction measurements.

Table 2. Relative Weights of the Six Most Abundant Isomers of Tetrahydrofurfuryl Alcohol at Room Temperature (Using Enthalpy Values)

	MP2/cc-pVTZ	MP2/aug-cc-pVDZ	34
A	0.37	0.32	0.84 ± 0.08
B	0.13	0.16	0.16 ± 0.08
C	0.37	0.36	
D	0.11	0.14	
E	0.00	0.01	
F	0.01	0.01	

Examination of the ground-state MOs shows that the highest occupied molecular orbital (HOMO) 28a is mainly the "out-of-plane" lone pair of the ring oxygen atom n(O). Depending on the conformation, this orbital is delocalized with large contributions of the neighboring σ(CH) MOs. The second-highest occupied molecular orbital (HOMO-1) 27a is essentially the OH oxygen lone pair n(OH) with contributions from the other σ bonds. The lowest unoccupied molecular orbital (LUMO) is mainly of σ^*(OH) antibonding character, with significant contributions of the σ^*(CH), depending on the geometry of the conformer. These orbitals are shown as Supporting Information together with the Cartesian coordinates of the atoms for the calculated geometries.

The two lowest vertical ionization energies (VIEs), which are needed to calculate the quantum defects associated with transitions to Rydberg orbitals, have been experimentally determined in this study (see section 5.1), using PES, to be 9.62 eV $(28a)^{-1}$ and 10.39 eV $(27a)^{-1}$, respectively. (See also refs 9, 10, and 14.)

3. EXPERIMENTAL DETAILS

3.1. THFA Sample. The liquid sample used in both the VUV measurements and the PES experiment was purchased from Sigma-Aldrich, with a stated purity of 99%. The sample was degassed by a repeated freeze−pump−thaw cycle in both sets of experiments.

3.2. VUV Photoabsorption. The high-resolution VUV photoabsorption measurements were performed using the UV1 beamline of the ASTRID synchrotron facility at Aarhus University, Denmark. (See Figure 1 for the present results.) A detailed description of the apparatus can be found elsewhere,[35] so only a brief description will be given here. Synchrotron radiation passes through a static gas sample, and a

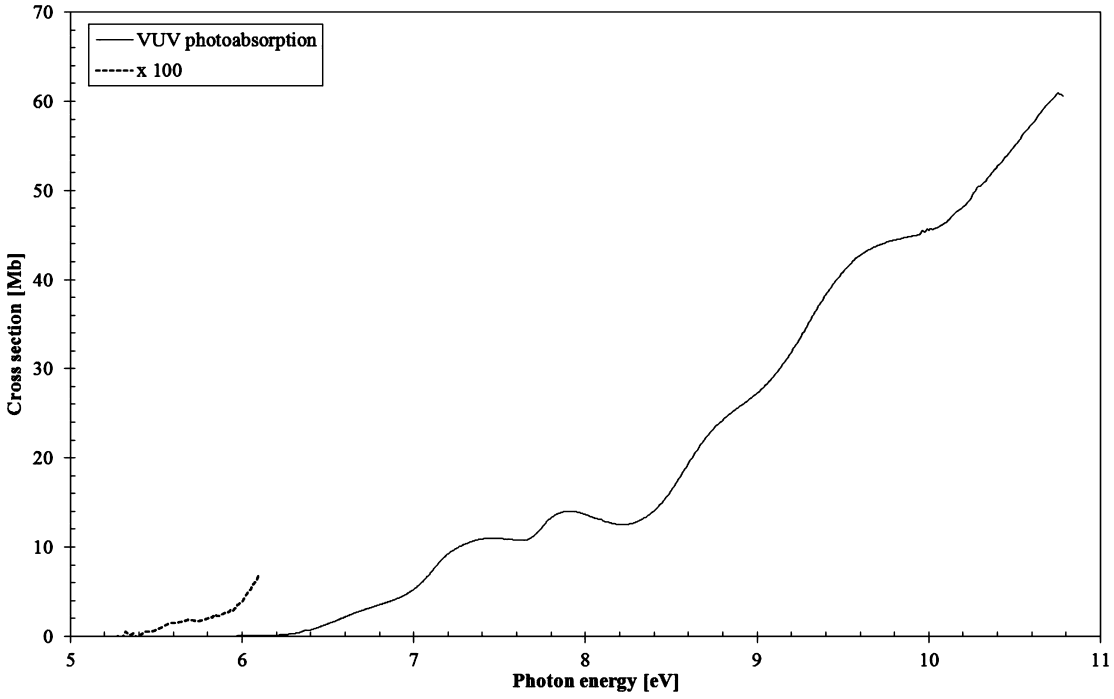

Figure 1. High-resolution VUV photoabsorption spectrum of tethrahydrofurfuryl alcohol in the 5.0−11.0 eV photon energy range.

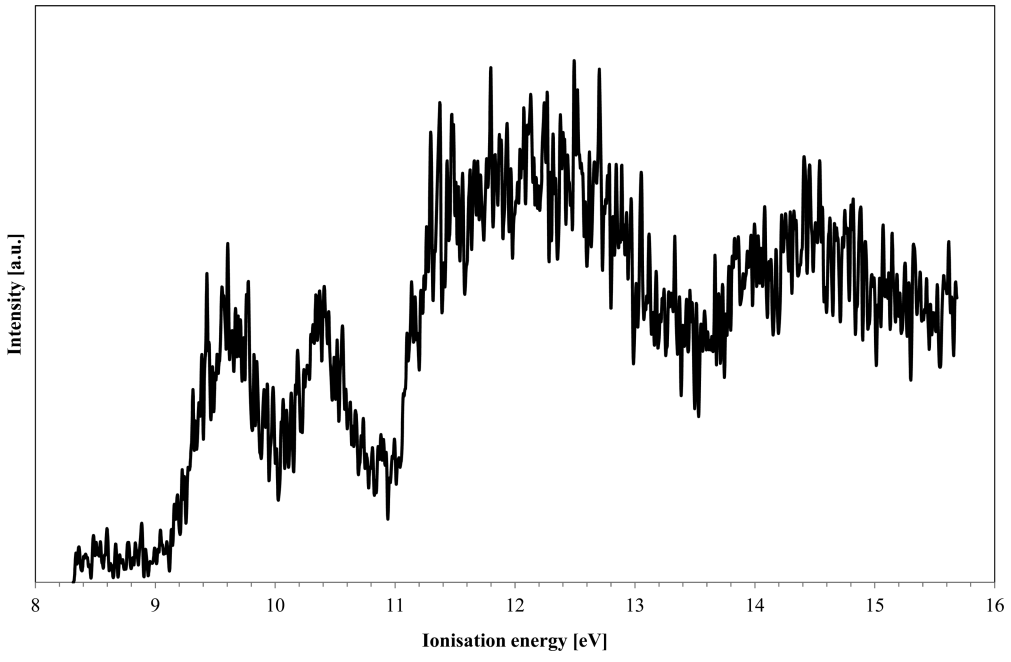

Figure 2. He(I) photoelectron spectrum of THFA in the 8.0−16 eV binding energy region.

photomultiplier is used to measure the transmitted light intensity. The incident wavelength is selected using a toroidal dispersion grating with 2000 lines/mm providing a resolution of 0.1 nm, corresponding to 3 meV at the midpoint of the energy range studied. For wavelengths below 200 nm (energies above 6.20 eV), the small gap between the photomultiplier and the exit window of the gas cell was evacuated to prevent any absorption by molecular oxygen in the air contributing to the spectrum. The sample pressure is measured using a capacitance manometer (Baratron). To ensure that the data are free of any saturation effects, we measured the absorption cross sections over the pressure range 0.02 to 1.00 Torr, with typical attenuations of <30%. The synchrotron beam ring current was monitored throughout the collection of each spectrum, and background scans were recorded with the cell evacuated. Absolute photoabsorption cross sections are then obtained using the Beer−Lambert attenuation law: $I_t = I_0 \exp(-n\sigma x)$, where I_t is the radiation intensity transmitted through the gas sample, I_0 is that through the evacuated cell, n is the molecular number density of the sample gas, σ is the absolute photoabsorption cross section, and x is the absorption path length (25 cm). The accuracy of the cross section is estimated to be ±5%. Only when absorption by the sample is very weak

dx.doi.org/10.1021/jp501634w | J. Phys. Chem. A 2014, 118, 6425−6434

Table 3. Calculated Vertical Excitation Energies (EOM-CCSD/aug-cc-pVTZ+R) (eV) and Oscillator Strengths Compared with the Present Experimental VUV Photoabsorption Cross Sections of Tetrahydrofurfuryl Alcohol, $C_5H_{10}O_2$: Isomer A

state	E (eV)	f_L	$\langle r^2 \rangle$[a]	HOMO (28a)	HOMO-1 (27a)	mixed character	exp. (eV)[b]	cross section (Mb)
1 ^{1}A			100					
2 ^{1}A	6.613	0.0075	142	3s/σ*(OH)			6.74(5)	3.18
3 ^{1}A	6.974	0.0037	145	3p/σ*(OH)				
4 ^{1}A	7.117	0.0028	149			HOMO → 3s/σ*(OH) + HOMO-1 → 3s/σ*(OH)		
5 ^{1}A	7.287	0.0070	158	3p/σ*(OH)				
6 ^{1}A	7.409	0.0204	169	3p/σ*(CH)			7.20(4)	9.30
7 ^{1}A	7.626	0.0264	165			HOMO → 3p/σ*(CH)/σ*(OH) + HOMO-1 → 3p	7.44(6)	10.98
8 ^{1}A	7.789	0.0105	170			HOMO → 3d + HOMO-1 → 3p/σ*(CH)/σ*(OH)		
9 ^{1}A	7.898	0.0220	195	3d			7.91(3)	14.03
10 ^{1}A	7.925	0.0036	200	3d				
11 ^{1}A	8.005	0.0058	201	3d				
12 ^{1}A	8.054	0.0049	193			HOMO → 4s + HOMO-1 → 3p	7.91(3)	14.03
13 ^{1}A	8.136	0.0050	222			HOMO → 3d + HOMO-1 → 3p		
14 ^{1}A	8.217	0.0005	285	4p				
15 ^{1}A	8.240	0.0005	246			HOMO → 4p + HOMO-1 → 3p		

[a]Mean value of r^2 (electronic radial spatial extents). [b]Last decimal of the energy value is given in brackets for these less-resolved features.

Table 4. Calculated Vertical Excitation Energies (EOM-CCSD/aug-cc-pVTZ+R) (eV) and Oscillator Strengths Compared with the Present Experimental VUV Photoabsorption Cross Sections of Tetrahydrofurfuryl Alcohol, $C_5H_{10}O_2$: Isomer B

state	E (eV)	f_L	$\langle r^2 \rangle$[a]	HOMO (28a)	HOMO-1 (27a)	mixed character	exp. (eV)[b]	cross section (Mb)
1 ^{1}A			102					
2 ^{1}A	6.615	0.00424	144	3s/σ*(CH)/σ*(OH)			6.74(5)	3.18
3 ^{1}A	7.005	0.00256	151	3p				
4 ^{1}A	7.077	0.00150	150	3p/σ*(OH)				
5 ^{1}A	7.221	0.00403	166	3p/σ*(CH)			7.20(4)	9.30
6 ^{1}A	7.528	0.01034	165			HOMO → 3d + HOMO-1 → 3s	7.44(6)	10.98
7 ^{1}A	7.737	0.00809	181	3d				
8 ^{1}A	7.816	0.06075	179			HOMO → 3d + HOMO-1 → 3p	7.91(3)	14.03
9 ^{1}A	7.878	0.00361	202	3d				
10 ^{1}A	7.975	0.00376	213	3d				
11 ^{1}A	8.042	0.00830	215			HOMO → 3d + HOMO-1 → 3p		
12 ^{1}A	8.098	0.00743	202			HOMO → 3d/σ*(OH) + HOMO-1 → 3p/σ*(OH)		
13 ^{1}A	8.133	0.00233	283	4s				
14 ^{1}A	8.204	0.00568	209			HOMO → 4p + HOMO-1 → 3d		
15 ^{1}A	8.311	0.00150	372	4p				

[a]Mean value of r^2 (electronic radial spatial extents). [b]Last decimal of the energy value is given in brackets for these less-resolved features.

($I_0 \approx I_t$) does the error significantly increase as a percentage of the measured cross section.

3.3. Photoelectron Spectroscopy. He(I) (21.22 eV) photoelectron spectra of THFA (see Figure 2 for the present results) were recorded at the Université de Liège, Belgium. The apparatus employed has been described in detail previously.[36] In brief, however, the spectrometer consists of a 180° cylindrical electrostatic analyzer with a mean radius of 5 cm. The analyzer is used in constant energy pass mode. The incident photons are produced by a DC discharge in a two-stage differentially pumped lamp. The energy scale was calibrated using the well-known argon lines ($^2P_{3/2}$ = 15.760 eV and $^2P_{1/2}$ = 15.937 eV),[37,38] and the resolution of the present spectrum is measured from the full width at half-maximum (fwhm) of the Ar peaks to be 22 meV in the presence of THFA. The intensities in the spectrum were corrected for the transmission of the analyzing system. The accuracy of the energy scale is estimated to be ±2 meV.

4. COMPUTATIONAL METHODS

Ab initio calculations were performed to determine the geometry and excitation energies of the neutral molecules (see Tables 3−9) and the VIE (Tables 10 and 11) using the MOLPRO program.[39] The geometry was optimized at the MP2 level using Dunning's cc-pVTZ and aug-cc-pVDZ atomic orbitals basis sets.[40] Six conformers, labeled A−F following Borisenko et al.,[34] were studied. The electronic spectra were computed at the equation of motion-coupled cluster with singles and doubles (EOM-CCSD) level.[41] For this, the aug-cc-pVDZ basis set was used, and a set of (6s6p5d) diffuse functions, taken from Kaufmann et al.,[42] was added on the C_2 carbon atom for a better description of Rydberg states. The oscillator strengths were obtained using the length gauge. Finally, the lowest VIEs were also calculated, using partial third order (P3) propagation and outer valence green function (OVGF)[43] calculations,[44] as implemented in the Gaussian 09 package.[45]

dx.doi.org/10.1021/jp501634w | J. Phys. Chem. A 2014, 118, 6425−6434

Table 5. Calculated Vertical Excitation Energies (EOM-CCSD/aug-cc-pVTZ+R) (eV) and Oscillator Strengths Compared with the Present Experimental VUV Photoabsorption Cross Sections of Tetrahydrofurfuryl Alcohol, $C_5H_{10}O_2$: Isomer C

state	E (eV)	f_L	$\langle r^2 \rangle$[a]	HOMO (28a)	HOMO-1 (27a)	mixed character	exp. (eV)[b]	cross section (Mb)
1 ^{1}A			100					
2 ^{1}A	6.709	0.01336	142	3s/σ*(OH)			6.74(5)	3.18
3 ^{1}A	7.044	0.00914	138			HOMO-1 → 3s/σ*(OH) + HOMO → 3p		
4 ^{1}A	7.208	0.01732	150			HOMO-1 → 3s/σ*(OH) + HOMO → 3p/σ*(OH)	7.44(6)	10.98
5 ^{1}A	7.419	0.03541	164	3p/σ*(CH)/σ*(OH)			7.20(4)	9.30
6 ^{1}A	7.549	0.01465	170	3p				
7 ^{1}A	7.694	0.01820	167			HOMO → 3d + HOMO-1 → 3p/σ*(OH)		
8 ^{1}A	7.873	0.00509	170	3d				
9 ^{1}A	7.987	0.00461	185	3d				
10 ^{1}A	8.029	0.00612	191	3d				
11 ^{1}A	8.106	0.01114	199			HOMO → 3d + HOMO-1 → 3p	7.91(3)	14.03
12 ^{1}A	8.112	0.00162	202	3d				
13 ^{1}A	8.250	0.00411	204			HOMO → 3d + HOMO-1 → 3p		
14 ^{1}A	8.303	0.00160	274	3d				
15 ^{1}A	8.335	0.00118	268	4s				

[a]Mean value of r^2 (electronic radial spatial extents). [b]Last decimal of the energy value is given in brackets for these less-resolved features.

Table 6. Calculated Vertical Excitation Energies (EOM-CCSD/aug-cc-pVTZ+R) (eV) and Oscillator Strengths Compared with the Present Experimental VUV Photoabsorption Cross Sections of Tetrahydrofurfuryl Alcohol, $C_5H_{10}O_2$: Isomer D

state	E (eV)	f_L	$\langle r^2 \rangle$[a]	HOMO (28a)	HOMO-1 (27a)	mixed character	exp. (eV)[b]	cross section (Mb)
1 ^{1}A			102					
2 ^{1}A	6.601	0.00574	146	3s/σ*(OH)			6.74(5)	3.18
3 ^{1}A	6.929	0.00719	148	3p/σ*(CH)/σ*(OH)				
4 ^{1}A	7.116	0.01659	158	3p			7.20(4)	9.30
5 ^{1}A	7.170	0.00792	166	3p				
6 ^{1}A	7.465	0.03651	158			HOMO-1 → 3s + HOMO → 3p	7.44(6)	10.98
7 ^{1}A	7.676	0.01069	179	3d				
8 ^{1}A	7.759	0.01607	180			HOMO → 3d + HOMO-1 → 3p	7.91(3)	14.03
9 ^{1}A	7.842	0.00056	199	3d				
10 ^{1}A	7.920	0.00017	205	3d				
11 ^{1}A	7.992	0.00234	200			HOMO → 4s + HOMO-1 → 3p		
12 ^{1}A	8.055	0.00873	200			HOMO → 4p + HOMO-1 → 3d		
13 ^{1}A	8.096	0.00657	262	3d				
14 ^{1}A	8.146	0.00528	223			HOMO → 4p + HOMO-1 → 3p		
15 ^{1}A	8.272	0.00476	381	4p				

[a]Mean value of r^2 (electronic radial spatial extents). [b]Last decimal of the energy value is given in brackets for these less-resolved features.

5. ELECTRONIC STATE SPECTROSCOPY: RESULTS AND DISCUSSION

The present absolute VUV photoabsorption cross section of THFA is shown in Figure 1, extending from 5.0 to 10.8 eV. The major absorption bands centered at ∼5.7, 6.7, 7.2, 7.4, 7.9, and 8.9 eV can be classified mainly as a mixture of Rydberg-valence transitions due to the promotion of an electron from the HOMO to the LUMO. Indeed, as shown in Tables 3−8, the lack of symmetry in THFA allows a mixing between the n = 3 Rydberg and the σ* (OH and CH) valence MOs. This mixing also depends on the conformation of the molecule. It should be noted that in THF,[15] where two conformers of C_2 and C_s symmetry are present, such a mixing does not occur. Tables 3−8 nevertheless show that all transitions below ∼8.3 eV are mainly Rydberg, with no "pure" σ* character. This is confirmed by a visual examination of the target MO and the $\langle r^2 \rangle$ value, which is for all transitions above the 100 au^2 of the ground state. This can also be checked theoretically by removing the diffuse atomic orbitals in the basis set (i.e., using the cc-pVDZ basis set). For the four most abundant conformers, the first transition, corresponding to HOMO → σ*(OH), is predicted between 8.1 and 8.3 eV (shown as Table I in the Supporting Information), close to the first IE. The oscillator strengths remain weak (∼0.01), which can be rationalized by the weak overlap between the HOMO and the σ*(OH) MO. As expected, the $\langle r^2 \rangle$ value remains ∼100 au^2.

Tables 3−8 also show a tentative assignment of the observed features based on the calculations. In contrast with THF,[15] where a distinct vibrational structure is observed, THFA shows only broad features, obviously because of the contribution of several of its conformers. The feature at ∼9.8 eV can be associated with the lowest ionic state of THFA. Nevertheless, data obtained from experiment are in a reasonably good agreement with theoretical predictions. In addition, for the first time, the photoabsorption spectrum was measured above 9.9 eV, thus extending the data over the lowest ionization region. Of relevance is the very weak experimental feature at ∼5.7 eV, which is not predicted by the calculations. One possible explanation could be that this feature is due to a singlet−triplet

dx.doi.org/10.1021/jp501634w | J. Phys. Chem. A 2014, 118, 6425−6434

Table 7. Calculated Vertical Excitation Energies (EOM-CCSD/aug-cc-pVTZ+R) (eV) and Oscillator Strengths Compared with the Present Experimental VUV Photoabsorption Cross Sections of Tetrahydrofurfuryl Alcohol, $C_5H_{10}O_2$: Isomer E

state	E (eV)	f_L	$\langle r^2 \rangle$[a]	HOMO (28a)	HOMO-1 (27a)	HOMO-2 (26a)	mixed character	exp. (eV)[b]	cross section (Mb)
1 ^{1}A			97						
2 ^{1}A	6.579	0.00413	137	3s				6.74(5)	3.18
3 ^{1}A	6.760	0.00395	135		3s/σ^*(OH)			6.74(5)	3.18
4 ^{1}A	6.957	0.00131	138	3p					
5 ^{1}A	7.170	0.00241	153	3p/σ^*(CH)/σ^*(OH)				7.20(4)	9.30
6 ^{1}A	7.278	0.00164	144	3p/σ^*(CH)					
7 ^{1}A	7.538	0.00802	152	3d/σ^*(CH)/σ^*(OH)					
8 ^{1}A	7.929	0.04036	156	3d/σ^*(CH)/σ^*(OH)				7.91(3)	14.03
9 ^{1}A	7.982	0.01561	161	3d/σ^*(CH)/σ^*(OH)					
10 ^{1}A	8.089	0.00325	156	3d					
11 ^{1}A	8.178	0.03403	138				HOMO-1 → 3s/σ^*(OH) + HOMO → 3d		
12 ^{1}A	8.192	0.00239	147				HOMO → 3d + HOMO-1 → 3s/σ^*(OH)		
13 ^{1}A	8.277	0.02540	137		3p/σ^*(OH)			7.91(3)	14.03
14 ^{1}A	8.406	0.00380	137		3p				
15 ^{1}A	8.478	0.01212	136			3s			

[a]Mean value of r^2 (electronic radial spatial extents). [b]Last decimal of the energy value is given in brackets for these less-resolved features.

Table 8. Calculated Vertical Excitation Energies (EOM-CCSD/aug-cc-pVTZ+R) (eV) and Oscillator Strengths Compared with the Present Experimental VUV Photoabsorption Cross Sections of Tetrahydrofurfuryl Alcohol, $C_5H_{10}O_2$: Isomer F

state	E (eV)	f_L	$\langle r^2 \rangle$[a]	HOMO (28a)	HOMO-1 (27a)	exp. (eV)[b]	cross section (Mb)
1 ^{1}A			97				
2 ^{1}A	6.584	0.00276	147	3s/σ^*(CH)		6.74(5)	3.18
3 ^{1}A	6.750	0.00403	136		3s/σ^*(OH)	6.74(5)	3.18
4 ^{1}A	6.952	0.01628	152	3p/σ^*(CH)/σ^*(OH)		7.20(4)	9.30
5 ^{1}A	7.179	0.00205	170	3p/σ^*(OH)			
6 ^{1}A	7.219	0.01000	167	3p			
7 ^{1}A	7.538	0.01104	178	3d/σ^*(OH)		7.91(3)	14.03
8 ^{1}A	7.791	0.00947	201	3d/σ^*(OH)			
9 ^{1}A	7.838	0.00396	209	3d			
10 ^{1}A	7.875	0.00466	215	3d			
11 ^{1}A	7.898	0.00308	213	3d			
12 ^{1}A	8.065	0.00320	330	4s			
13 ^{1}A	8.080	0.02151	159		3p/σ^*(CH)/σ^*(OH)	7.91(3)	14.03
14 ^{1}A	8.181	0.00417	389	4p			
15 ^{1}A	8.199	0.01888	159		3p/σ^*(CH)/σ^*(OH)		

[a]Mean value of r^2 (electronic radial spatial extents). [b]Last decimal of the energy value is given in brackets for these less-resolved features.

Table 9. Calculated Vertical Excitation Energies (in eV) and Oscillator Strengths (f_L) for the THFA Conformers, Using TDDFT and EOM-CCSD[a]

	A			B			C		
conformer	E(T)	E(S)	f_L(S)	E(T)	E(S)	f_L(S)	E(T)	E(S)	f_L(S)
CAM-B3LYP	6.447	6.575	0.0079	6.449	6.577	0.0037	6.517	6.688	0.0118
ωB97X-D	6.639	6.736	0.0077	6.636	6.735	0.0038	6.707	6.837	0.0120
M06-2X	6.568	6.684	0.0077	6.582	6.671	0.0025	6.649	6.798	0.0094
EOM-CCSD[b]		6.613	0.0075		6.615	0.0042		6.709	0.0134
EOM-CCSD[c]	6.541	6.640	0.0079	6.543	6.640	0.0045	6.602	6.736	0.0140
	D			E			F		
conformer	E(T)	E(S)	f_L(S)	E(T)	E(S)	f_L(S)	E(T)	E(S)	f_L(S)
CAM-B3LYP	6.452	6.583	0.0057	6.275	6.534	0.0062	6.280	6.556	0.0025
ωB97X-D	6.632	6.739	0.0055	6.504	6.686	0.0052	6.509	6.733	0.0026
M06-2X	6.584	6.676	0.0040	6.494	6.651	0.0046	6.499	6.710	0.0026
EOM-CCSD[b]		6.601	0.0057		6.579	0.0041		6.584	0.0028
EOM-CCSD[c]	6.452	6.583	0.0057	6.275	6.534	0.0062	6.280	6.556	0.0025

[a]E(T) and E(S) are energies for triplet and singlet states, respectively. [b]Molpro, with additional diffuse functions (aug-cc-pVDZ+R basis set). [c]Gaussian 09 (aug-cc-pVDZ basis set).

dx.doi.org/10.1021/jp501634w | J. Phys. Chem. A 2014, 118, 6425−6434

Table 10. Calculated Vertical Ionization Energies (VIE) (in eV) and Intensities (Pole Strength) for THFA (cc-pVTZ level), $C_5H_{10}O_2$, with the OVGF Method and cc-pVTZ Basis Set

	$28a^{-1}$		$27a^{-1}$		$26a^{-1}$		$25a^{-1}$		$24a^{-1}$		$23a^{-1}$	
conformer	IE	PS	IE	PS	IE	PS	IE	PS	IE	PS	IE	PS
A	10.024	0.911	10.667	0.911	11.930	0.913	11.995	0.909	12.478	0.909	12.765	0.910
B	9.9200	0.910	10.948	0.911	11.817	0.911	11.863	0.908	12.406	0.914	12.689	0.908
C	10.131	0.911	10.726	0.911	11.885	0.914	12.039	0.909	12.328	0.908	12.695	0.912
D	9.9020	0.911	10.883	0.912	11.808	0.909	12.057	0.912	12.282	0.911	12.675	0.908
E	9.8140	0.911	10.938	0.914	11.426	0.908	11.876	0.913	12.148	0.911	12.461	0.908
F	9.8490	0.910	10.910	0.915	11.489	0.908	11.871	0.913	12.181	0.909	12.427	0.907
exp. value	9.62 ± 0.05		10.39 ± 0.05									
exp. value[9]	9.81		10.60									
exp. value[14]	9.8		10.7									
	$22a^{-1}$		$21a^{-1}$		$20a^{-1}$		$19a^{-1}$		$18a^{-1}$		$17a^{-1}$	
conformer	IE	PS	IE	PS	IE	PS	IE	PS	IE	PS	IE	PS
A	12.701	0.908	13.891	0.909	14.818	0.906	15.343	0.906	15.442	0.903	16.100	0.904
B	13.745	0.909	13.922	0.907	14.704	0.907	14.923	0.905	15.276	0.905	16.497	0.903
C	12.597	0.908	14.172	0.908	14.611	0.906	15.051	0.907	15.913	0.904	16.343	0.903
D	13.400	0.910	14.256	0.907	14.862	0.907	14.750	0.905	15.384	0.906	16.466	0.902
E	13.262	0.909	14.039	0.908	14.471	0.907	14.613	0.904	15.683	0.904	16.478	0.899
F	13.144	0.911	14.029	0.907	14.455	0.906	14.953	0.904	15.412	0.905	15.412	0.905

Table 11. Calculated Vertical Ionization Energies (VIE) (in eV) and Intensities (Pole Strength) for THFA (cc-pVTZ level), $C_5H_{10}O_2$, with the P3 Method and cc-pVTZ Basis Set

	$28a^{-1}$		$27a^{-1}$		$26a^{-1}$		$25a^{-1}$		$24a^{-1}$		$23a^{-1}$	
conformer	IE	PS	IE	PS	IE	PS	IE	PS	IE	PS	IE	PS
A	10.528	0.923	11.075	0.921	12.236	0.921	12.389	0.919	12.859	0.920	13.132	0.902
B	10.408	0.922	11.415	0.921	12.148	0.920	12.301	0.920	12.612	0.921	13.110	0.919
C	10.636	0.923	11.164	0.922	12.134	0.921	12.440	0.920	12.749	0.919	13.019	0.921
D	10.388	0.922	11.325	0.922	12.193	0.919	12.399	0.921	12.595	0.920	13.111	0.919
E	10.301	0.922	11.302	0.923	11.880	0.919	12.142	0.921	12.434	0.919	12.885	0.919
F	10.357	0.922	11.255	0.923	11.912	0.919	12.128	0.921	12.532	0.919	12.875	0.919
exp. value	9.62 ± 0.05		10.39 ± 0.05									
exp. value[9]	9.81		10.60									
exp. value[14]	9.8		10.7									
	$22a^{-1}$		$21a^{-1}$		$20a^{-1}$		$19a^{-1}$		$18a^{-1}$		$17a^{-1}$	
conformer	IE	PS	IE	PS	IE	PS	IE	PS	IE	PS	IE	PS
A	13.118	0.919	14.278	0.919	15.153	0.916	15.854	0.916	15.967	0.914	16.639	0.915
B	14.074	0.918	14.329	0.918	15.003	0.916	15.379	0.917	15.779	0.915	16.997	0.913
C	13.015	0.919	14.654	0.920	14.912	0.916	15.362	0.916	16.457	0.915	16.867	0.914
D	13.701	0.918	14.719	0.918	15.128	0.916	15.125	0.916	15.995	0.917	16.917	0.912
E	13.686	0.920	14.395	0.917	14.795	0.916	15.062	0.916	16.139	0.914	17.070	0.912
F	13.512	0.920	14.447	0.917	14.756	0.915	15.394	0.916	15.922	0.915	17.036	0.913

transition, although this is forbidden in the electric dipole approximation. Because MOLPRO is not able to calculate triplet transitions, we calculated (for all conformers) the lowest singlet and triplet transitions using the TDDFT method, as implemented in Gaussian 09, together with the aug-cc-pVDZ basis. The choice of the functionals (CAM-B3LYP, M06-2X, and ωB97X-D) was based on a recent review (figure 3 in ref 46). For the three functionals, the first singlet transition energies and oscillator strengths of all conformers (Table 9) are in very good agreement with the EOM-CCSD results shown in Table 3. The corresponding triplet transitions are all predicted to be in the range 6.3 to 6.7 eV (Table 9). We also recalculated the first singlet and triplet transitions using the EOM-CCSD method implemented in Gaussian 09 and obtained values similar to TDDFT. For all methods and conformers, the triplet transitions are very close in energy to the singlet. Therefore, we conclude that the observed feature at ~5.7 eV does not seem to correspond to a triplet transition. Such a feature therefore remains as yet unassigned.

Our photoelectron spectrum, shown in Figure 2, proposes the lowest VIE at 9.62 ± 0.05 and 10.39 ± 0.05 eV, in very good agreement with the theoretical calculations presented both in this work (see Tables 10 and 11) and the previously determined experimental photoelectron and dynamical (e, 2e) data.[9,10,14] The calculated VIEs are presented in Tables 10 and 11. The measured lowest vertical IEs of THFA agree reasonably well with the OVGF theoretical predictions. As far as the P3 method is concerned, however, the IEs are noticeably larger by ~0.5 eV.

5.1. He(I) Photoelectron Data. The photoelectron spectrum of THFA has already been reported by Allan and coworkers,[9] with values for the two lowest VIE being derived.

dx.doi.org/10.1021/jp501634w | J. Phys. Chem. A 2014, 118, 6425−6434

In the first electronic band, the point of maximum intensity was found at 9.81 eV, corresponding to the removal of an n(O) electron, while the next feature at 10.39 eV was due to the removal of an electron from n(OH). In the present experiment, we suggest values of 9.62 ± 0.05 and 10.39 ± 0.05 eV. The calculated values, shown in Tables 10 and 11, demonstrate that the six isomers all have very similar IEs. All theoretical results predict slightly higher VIE when compared with the measured data.

5.2. Rydberg Transitions. The VUV spectrum above 6.0 eV consists of diffuse absorption features extending to the lowest IEs. Computation revealed that it originates mainly from transitions from the HOMO (n(O)) and HOMO-1 (n(OH)) orbitals to the lowest Rydberg states. Ab initio calculations show that all six conformers will contribute to these transitions according to their Boltzmann factors (see Table 2) with the calculated energies for such transitions to the n = 3 term together with their oscillator strengths (f_L) being shown in Tables 3−9. The experimental IE values in Tables 10 and 11 are used to help tentatively assign the Rydberg series. The proposed Rydberg structures are presented in Table 12. The

Table 12. Energies (eV), Quantum Defects, and Assignments of the ns, np, and nd Rydberg Series Converging to the Ionic Electronic Ground $(28a)^{-1}$ and First $(27a)^{-1}$ Excited States of THFA, $C_5H_{10}O_2$

vertical energy	quantum defect (δ)	assignment
IE_1 = 9.62 eV		
6.74(5)[a]	0.82	3s
7.20(4)[a]	0.62	3p
7.91(3)[a]	0.17	3d
IE_2 = 10.39 eV		
7.44(6)[a]	0.85	3s
7.91(3)[a]	0.65	3p
8.90(0)[a]	−0.02	3d

[a]Indicates a broad structure. (The last decimal of the energy value is given in brackets for these less-resolved features.)

peak positions, E_n, have been tested using the Rydberg formula: $E_n = E_i - R/(n - \delta)^2$, where E_i is the IE, n is the principal quantum number of the Rydberg orbital of energy E_n, R is the Rydberg constant (13.61 eV), and δ is the quantum defect resulting from the penetration of the Rydberg orbital into the core. Regarding the ionization of the oxygen (in the ring) lone-pair n(O) electrons, the lowest energy (6.74(5) eV) is tentatively assigned to the Rydberg transition (3s ← n(O), 28a) with a quantum defect δ = 0.82, whereas the np and nd series are associated with the peaks at 7.20(4) eV (δ = 0.62) and 7.91(3) eV (δ = 0.17), respectively. (See Table 12.) As far as the Rydberg series converging to the first ionic excited state are concerned, the n = 3 members have been obtained for ns, np, and nd with quantum defects of δ = 0.85, 0.65, and −0.02, respectively. (Again, see Table 12.) Because of the broad and structureless nature of the absorption bands, no higher order members of these Rydberg series have been proposed.

Note that the clear increase in the absorption with energy, in the range above ∼7.0 eV, may be related to low-lying predissociative or dissociative excited neutral states.

5.3. Valence State Spectroscopy of THFA. Calculations predict that the region above 6.0 eV in the VUV photoabsorption spectrum mainly contains Rydberg transitions. The calculated values for the energies and oscillator strengths in this region for the six conformers are shown in Tables 3−9. However, we note that for isomer E (see Table 7) the absorption band centered at 6.74(5) eV clearly has mixed valence/Rydberg character with a maximum absolute cross section of 3.18 Mb, albeit this isomer contributes to only ∼1% of the total photoabsorption intensity. The rather high calculated intensity is primarily due to the important valence σ^* character of the MO, so that this transition should be labeled as (σ^*(OH) ← n(OH)).

Because of the large increase in the cross section (>8 eV), it was difficult to identify all possible valence transitions as well as any possible underlying dissociative states predicted by the calculations.

5.4. Absolute Photoabsorption Cross Sections. The present optical measurements were carried out in the pressure range 0.02 to 1.00 Torr and reveal no evidence of changes in the absolute cross sections or peak energies as a function of pressure. Thus, we believe the present spectra are free of any saturation effects. Previous absolute VUV photoabsorption cross sections of THFA are restricted to the wavelength ranges 125−248 nm (9.9−6.2 eV).[32] Dickinson and Johnson[32] reported cross sections of magnitude ∼6.64 Mb (157 nm, 7.89 eV) comparatively lower than the present respective value of 14.03 Mb. We believe that this difference may be attributed to the resolution of each apparatus; however, other factors such as the role of saturation in the other data set may also lead to the observation of lower cross sections by the previous authors. Furthermore, the general level of agreement of previous cross sections measured at the ASTRID beamline with the most precise independent data available in the literature (see Eden et al.[47] and references therein) suggests that the present THFA cross sections can be relied upon across the energy range studied up to 10.8 eV. (See Figure 1.)

6. CONCLUSIONS

The present work provides the first complete study of the VUV electronic spectra of THFA and provides the most reliable set of absolute photoabsorption cross sections available between 5.0 to 10.8 eV. The observed structure has been assigned to Rydberg transitions with slight valence (σ^*(OH) and σ^*(CH)) character, on the basis of comparisons with the present and past ab initio calculations of vertical excitation energies and oscillator strengths for this molecule. The present theoretical results are therefore in good agreement with those from our experiments. The VIEs were found to be 9.62 ± 0.05 and 10.39 ± 0.05 eV, which are in good agreement with the values given previously[9,10,14] and with the calculated values using OVGF and P3 methods.

■ ASSOCIATED CONTENT

Supporting Information

HOMO, HOMO-1, and LUMO of THFA isomers plotted using the MOLDEN software as well as the geometries of ground state $\tilde{X}^1$ A state at the MP2/aug-cc-pVDZ level and MP2/cc-pVTZ level. This material is available free of charge via the Internet at http://pubs.acs.org.

■ AUTHOR INFORMATION

Corresponding Author

*Tel: (+351) 21 294 78 59. Fax: (+351) 21 294 85 49. E-mail: plimaovieira@fct.unl.pt.

Notes

The authors declare no competing financial interest.

■ ACKNOWLEDGMENTS

P.L.-V. acknowledges partial funding from the research grants PEst-OE/FIS/UI0068/2014 and PTDC/FIS-ATO/1832/2012 through FCT-MEC and together with M.-J.H.-F. acknowledges the financial support from the Portuguese−Belgian joint collaboration. The Patrimoine of the University of Liège, the Fonds National de la Recherche Scientifique, and the Fonds de la Recherche Fondamentale Collective of Belgium have supported this research. We acknowledge the beam time at the ISA synchrotron at Aarhus University, Denmark. We also acknowledge the financial support provided by the European Commission through the Access to Research Infrastructure action of the Improving Human Potential Programme, FP6-Transnational Access Programme IA-5F5:R113-CT-2004-506008. D.D. acknowledges support from the CaPPA project (Chemical and Physical Properties of the Atmosphere), funded by the French National Research Agency (ANR) through the PIA (Programme d'Investissement d'Avenir) under contract ANR-10-LABX-005 and access to the HPC resources of CINES under the allocation 2014-088620 made by GENCI. The Centre de Ressources Informatiques (CRI) of the Université Lille1 also provided computing time. D.B.J. thanks the Australian Research Council for financial support provided through a Discovery Early Career Research Award. Finally, M.J.B. also thanks the Australian Research Council for some financial support, while M.J.B. and M.C.A.L. acknowledge the Brazilian agency CNPq also for financial support.

■ REFERENCES

(1) Boudaïffa, B.; Cloutier, P.; Hunting, D.; Huels, M. A.; Sanche, L. Resonant Formation of DNA Strand Breaks by Low-Energy (3 to 20 eV) Electrons. *Science* **2000**, *287*, 1658−1660.

(2) Baccarelli, I.; Bald, I.; Gianturco, F. A.; Illenberger, E.; Kopyra, J. Electron-Induced Damage of DNA and its Components: Experiments and Theoretical Models. *Phys. Rep.* **2011**, *508*, 1−44.

(3) Prise, K. M.; O'Sullivan, J. M. Radiation-Induced Bystander Signalling in Cancer Therapy. *Nat. Rev. Cancer* **2009**, *9*, 351−360.

(4) Sanz, A. G.; Fuss, M. C.; Munoz, A.; Blanco, F.; Limão-Vieira, P.; Brunger, M. J.; Buckman, S. J.; García, G. Modelling Low Energy Electron and Positron Tracks for Biomedical Applications. *Int. J. Radiat. Biol.* **2012**, *88*, 71−76.

(5) Petrovic, Z. Lj.; Marjanovic, S.; Dujko, S.; Bankovic, A.; Malovic, G.; Buckman, S. J.; García, G.; White, R.; Brunger, M. J. On The Use of Monte Carlo Simulations to Model Transport of Positrons in Gases and Liquids. *Appl. Radiat. Isot.* **2014**, *83*, 148−154.

(6) Ptasinska, S.; Denifl, S.; Scheier, P.; Mark, T. D. Inelastic electron interaction (attachment/ionization) with deoxyribose. *J. Chem. Phys.* **2004**, *120*, 8505−8511.

(7) Almeida, D.; Ferreira da Silva, F.; García, G.; Limão-Vieira, P. Dynamic of negative ions in potassium-D-ribose collisions. *J. Chem. Phys.* **2013**, *139*, 114304.

(8) Vall-Llosera, G.; Huels, M. A.; Coreno, M.; Kivimäki, A.; Jakubowska, K.; Stankiewicz, M.; Rechlew, E. Photofragmentation of 2-deoxy-D-ribose Molecules in the Gas Phase. *ChemPhysChem* **2008**, *9*, 1020−1029.

(9) Ibanescu, B. C.; May, O.; Monney, A.; Allan, M. Electron-Induced Chemistry of Alcohols. *Phys. Chem. Chem. Phys.* **2007**, *9*, 3163−3173.

(10) Jones, D. B.; Builth-Williams, J. D.; Bellm, S. M.; Chiari, L.; Chaluvadi, H.; Madison, D. H.; Ning, C. G.; Lohmann, B.; Ingólfsson, O.; Brunger, M. J. Dynamical (e,2e) Investigations of Tetrahydrofuran and Tetrahydrofurfuryl Alcohol as DNA Analogues. *Chem. Phys. Lett.* **2013**, *572*, 32−37.

(11) Zecca, A.; Chiari, L.; García, G.; Blanco, F.; Trainotti, E.; Brunger, M. J. Total Cross-Sections for Positron and Electron Scattering From Alpha-Tetrahydrofurfuryl Alcohol. *New J. Phys.* **2011**, *13*, 063019.

(12) Brunger, M. J.; Buckman, S. J.; Sullivan, J. P.; Palihawadana, P.; Jones, D. B.; Chiari, L.; Pettifer, Z.; da Silva, G. B.; Lopes, M. C. A.; Duque, H. V.; et al. Recent Progress in Electron Scattering From Atoms and Molecules. *Am. Inst. Phys., Conf. Proc.* **2014**, *1588*, 71−77.

(13) Milosavljevic, A. R.; Kocisek, J.; Papp, P.; Kubala, D.; Marinkovic, B. P.; Mach, P.; Urban, J.; Matejcik, S. Electron Impact Ionization of Furanose Alcohols. *J. Chem. Phys.* **2010**, *132*, 104308.

(14) Bellm, S. M.; Builth-Williams, J. D.; Jones, D. B.; Chaluvadi, H.; Madison, D. H.; Ning, C. G.; Wang, F.; Ma, X. G.; Lohmann, B.; Brunger, M. J. Dynamical (e,2e) Studies of Tetrahydrofurfuryl Alcohol. *J. Chem. Phys.* **2012**, *136*, 244301.

(15) Giuliani, A.; Limão-Vieira, P.; Duflot, D.; Milosavljevic, A. R.; Marinkovic, B. P.; Hoffmann, S. V.; Mason, N. J.; Delwiche, J.; Hubin-Franskin, M.-J. Electronic States of Neutral and Ionized Tetrahydrofuran Studied by VUV Spectroscopy and ab initio Calculations. *Eur. Phys. J. D* **2009**, *51*, 97−108.

(16) Chiari, L.; Anderson, E.; Tattersall, W.; Machacek, J. R.; Palihawadana, P.; Makochekanwa, C.; Sullivan, J. P.; García, G.; Blanco, F.; McEachran.; et al. Total, Elastic, and Inelastic Cross Sections for Positron and Electron Collisions With Tetrahydrofuran. *J. Chem. Phys.* **2013**, *138*, 074301.

(17) Fuss, M. C.; Colmenares, R.; Sanz, A. G.; Munoz, A.; Oller, J. C.; Blanco, F.; Do, T. P. T.; Brunger, M. J.; Almeida, D.; Limão-Vieira, P.; et al. Electron Interactions With Tetrahydrofuran. *J. Phys. Conf. Ser.* **2012**, *373*, 012010.

(18) Duflot, D.; Flament, J. P.; Heinesch, J.; Hubin-Franskin, M.-J. The K-Shell Spectra of Tetrahydrofuran Studied by Electron Energy Loss Spectroscopy and ab initio Calculations. *Chem. Phys. Lett.* **2010**, *495*, 27−32.

(19) Dampc, M.; Linert, I.; Milosavljevic, A. R.; Zubek, M. Vibrational Excitation of Tetrahydrofuran by Electron Impact in the Low Energy Range. *Chem. Phys. Lett.* **2007**, *443*, 17−21.

(20) Dampc, M.; Milosavljevic, A. R.; Linert, I.; Marinkovic, B. P.; Zubek, M. Differential Cross Sections for Low-Energy Elastic Electron Scattering from Tetrahydrofuran in the Angular Range 20 Degrees-180 Degrees. *Phys. Rev. A* **2007**, *75*, 042710.

(21) Milosavljevic, A. R.; Blanco, F.; Sevic, D.; García, G.; Marinkovic, B. P. Elastic Scattering of Electrons From Tetrahydrofurfuryl Alcohol. *Eur. Phys. J. D* **2006**, *40*, 107−114.

(22) Sulzer, P.; Ptasinska, S.; Zappa, F.; Mielewska, B.; Milosavljevic, A. R.; Scheier, P.; Märk, T. D.; Bald, I.; Gohlke, S.; Huels, M. A.; et al. Dissociative Electron Attachment to Furan, Tetrahydrofuran, and Fructose. *J. Chem. Phys.* **2006**, *125*, 044304.

(23) Milosavljevic, A. R.; Giuliani, A.; Sevic, D.; Hubin-Franskin, M.-J.; Marinkovic, M. P. Elastic Scattering of Electrons From Tetrahydrofuran Molecule. *Eur. Phys. J. D* **2005**, *35*, 411−416.

(24) Milosavljevic, A. R.; Sevic, D.; Marinkovic, B. P. Electron Interaction With Deoxyribose Analogue Molecules in Gaseous Phase. *J. Phys. Conf. Ser.* **2008**, *101*, 012014.

(25) Almeida, D.; Ferreira da Silva, F.; Eden, S.; García, G.; Limão-Vieira, P. New Fragmentation Pathways in K-THF Collisions As Studied by Electron-Transfer Experiments: Negative Ion Formation. *J. Phys. Chem. A* **2014**, *118*, 690−696.

(26) Do, T. P. T.; Leung, M.; Fuss, M.; García, G.; Blanco, F.; Ratnavelu, K.; Brunger, M. J. Excitation of Electronic States in Tetrahydrofuran by Electron Impact. *J. Chem. Phys.* **2011**, *134*, 144302.

(27) Garland, N. A.; Brunger, M. J.; García, G.; de Urquijo, J.; White, R. D. Transport Properties of Electron Swarms in Tetrahydrofuran Under the Influence of an Applied Electric Field. *Phys. Rev. A* **2013**, *88*, 062712.

(28) Fuss, M.; Munoz, A.; Oller, J. C.; Blanco, F.; Almeida, D.; Limão-Vieira, P.; Do, T. P. D.; Brunger, M. J.; García, G. Electron-Scattering Cross Sections for Collisions With Tetrahydrofuran From 50 to 5000 eV. *Phys. Rev. A* **2009**, *80*, 052709.

(29) Giuliani, A.; Walker, I. C.; Delwiche, J.; Hoffmann, S. V.; Limão-Vieira, P.; Mason, N. J.; Heyne, B.; Hoebeke, M.; Hubin-Franskin, M.-J. The Electronic States of 2-Furanmethanol (Furfuryl Alcohol) Studied by Photon Absorption and Electron Impact Spectroscopies. *J. Chem. Phys.* **2003**, *119*, 7282−7288.
(30) Giuliani, A.; Delwiche, J.; Hoffmann, S. V.; Limão-Vieira, P.; Mason, N. J.; Hubin-Franskin, M.-J. 2-Methyl Furan: An Experimental Study of the Excited Electronic Levels by Electron Energy Loss Spectroscopy, Vacuum Ultraviolet Photoabsorption, and Photoelectron Spectroscopy. *J. Chem. Phys.* **2003**, *119*, 3670−3680.
(31) Walker, I. C.; Palmer, M. H.; Delwiche, J.; Hoffmann, S. V.; Limão-Vieira, P.; Mason, N. J.; Guest, M. F.; Hubin-Franskin, M.-J.; Heinesch, J.; Giuliani, A. The Electronic States of Isoxazole Studied by VUV Absorption, Electron Energy-Loss Spectroscopies and ab initio Multi-Reference Configuration Interaction Calculations. *Chem. Phys.* **2004**, *297*, 289−306.
(32) Dickinson, H. R.; Johnson, W. C., Jr. Optical-Properties of Sugars 0.2. Vacuum Ultraviolet Absorption of Model Compounds. *J. Am. Chem. Soc.* **1974**, *96*, 5050−5054.
(33) Papp, P.; Mach, P.; Urban, J.; Matejcik, S. Quantum-Chemical Calculations of the Products and Energies of Electron Induced Ionization of 2-Furanmethanol, Tetrahydro-and-3-Furanol. *Facta Univ., Ser.: Phys., Chem. Technol.* **2008**, *6*, 127−139.
(34) Borisenko, K. B.; Samdal, S.; Shishkov, I. F.; Vilkov, L. V. Molecular Structure and Conformations of Tetrahydrofurfuryl Alcohol From a Joint Gas-Phase Electron Diffraction and ab initio Molecular Orbital Investigation. *J. Mol. Struct.* **1998**, *448*, 29−41.
(35) Eden, S.; Limão-Vieira, P.; Hoffmann, S. V.; Mason, N. J. VUV Photoabsorption in CF_3X (X = Cl, Br, I) Fluoro-Alkanes. *Chem. Phys.* **2006**, *323*, 313−333.
(36) Delwiche, J.; Natalis, P.; Momigny, J.; Collin, J. E. On the Photoelectron Spectra of HBr and DBr. *J. Electron Spec. Relat. Phenom.* **1972**, *1*, 219−225.
(37) *Handbook of Chemistry and Physics*; Lide, D. R., Ed.; CRC Press: New York, 1992.
(38) Eland, J. H. D. *Photoelectron Spectroscopy*; Butterworth & Co Ltd.: London, 1984.
(39) Werner, H.-J.; Knowles, P. J.; Knizia, G.; Manby, F. R.; Schütz, M.; Celani, P.; Korona, T.; Lindh, R.; Mitrushenkov, A.; Rauhut, G. et al. *MOLPRO*, version 2012.1, a package of ab initio programs, see http://www.molpro.net.
(40) Dunning, T. H., Jr. Gaussian-Basis Sets For Use in Correlated Molecular Calculations 0.1. The Atoms Boron Through Neon and Hydrogen. *J. Chem. Phys.* **1989**, *90*, 1007−1023.
(41) Korona, T.; Werner, H.-J. Local Treatment of Electron Excitations in the EOM-CCSD Method. *J. Chem. Phys.* **2003**, *118*, 3006−3019.
(42) Kaufmann, K.; Baumeister, W.; Jungen, M. Universal Gaussian-Basis Sets For an Optimum Representation of Rydberg and Continuum Wavefunctions. *J. Phys. B* **1989**, *22*, 2223−2240.
(43) Ortiz, J. V.; Zakrzewski, V. G.; Dolgounircheva, O. *Conceptual Perspectives in Quantum Chemistry*; Calais, J.-L., Kryachko, E., Eds.; Kluwer Academic: Boston, 1997.
(44) Ferreira, A. M.; Seabra, G.; Dolgounitcheva, O.; Zakrzewski, V. G.; Ortiz, J. V. Application and Testing of Diagonal, Partial Third-Order Electron Propagator Approximation. In *Quantum Mechanical Prediction of Thermochemical Data*; Cioslowski, J., Ed.; Kluwer: Dordrecht, The Netherlands, 2001; p 131
(45) Frisch, M. J.; Trucks, G. W.; Schlegel, H. B.; Scuseria, G. E.; Robb, M. A.; Cheeseman, J. R.; Scalmani, G. ; Barone, V.; Mennucci, B.; Petersson, G. A. *Gaussian 09*, revision C.01; Gaussian, Inc.: Wallingford, CT, 2010.
(46) Laurent, A. D.; Jacquemin, D. TD-DFT Benchmarks: A Review. *Int. J. Quantum Chem.* **2013**, *113*, 2019−2039.
(47) Eden, S.; Limão-Vieira, P.; Hoffmann, S. V.; Mason, N. J. VUV Spectroscopy of CH_3Cl and CH_3I. *Chem. Phys.* **2007**, *331*, 232−244.